scientific reports

Check for updates

OPEN

IL-17A regulates airway remodelling in COPD through the PI3K/AKT/mTOR pathway

Ting Ding✉, Shunshun Zhao, Yanhui Gu, Guiqiang He, Yanzhu Lang, Ximin Rao, Jie Chen & Yao Ou-Yang✉

The airway and lung tissue inflammation and structural changes caused by COPD lead to persistent and irreversible airflow limitation in patients. Several studies have associated IL-17A with COPD airway inflammation and collagen deposition, while autophagy is essential for maintaining normal cell function. Based on these findings, we propose a hypothesis that IL-17 affecting the autophagy of macrophages through the PI3K/AKT/mTOR pathway may contribute to the regulation of the airway remodeling process in COPD. The COPD airway remodelling model was confirmed by pulmonary function tests and HE and Masson staining. IL-17A, IL-6 and CCL20 were detected by ELISA, autophagosomes (APs) were observed by transmission electron microscopy, and western blotting was used to detect PI3K/AKT/mTOR-related proteins, autophagy-related proteins and collagen. Immunofluorescence revealed colocalization of LC3 in mouse bronchial fibroblasts (MBFs). MBFs were isolated and cultured via lentiviral transfection, IL-17RA overexpression or silencing, and quantitative analysis of PI3K/AKT/mTOR pathway-related proteins and autophagy-related proteins via western blotting. The results validated the establishment of the COPD model. Increased IL-17A in the COPD airway and increased IL-6 and CCL20 expression were observed in the COPD mice supplemented with the autophagy inhibitor 3MA. Using TEM, we observed a significant reduction in the number of APs in the airways in both the COPD and 3MA groups. Moreover, the PI3K/AKT/mTOR pathway phospho-p-PI3K/PI3K, p-AKT/AKT, and p-mTOR/mTOR ratios were also increased in the COPD group. Moreover, as P62 increased, Beclin-1 and LC3II/I expression decreased correspondingly, while Collagen I and Collagen III also increased. In our study of cultured mouse MBFs, the results showed that overexpression (OE) virus-mediated transfection of MBFs overexpressing IL-17RA increased the p-PI3K/PI3K, p-AKT/AKT, and p-mTOR/mTOR ratios, increased the P62 content and reduced the expression of Beclin-1 and LC3II/I. However, compared with the OE group, the silencing (sh)-mediated transfection of MBFs with IL-17RA had almost opposite effects. Increased collagen production and the expression of IL-17A, IL-6 and CCL20 in the airways of COPD mice. Autophagy decreased, and the PI3K/AKT/mTOR pathway was activated in COPD airway tissue. In primary cultured MBFs from COPD mice, IL-17A combined with IL-17RA activates the PI3K/AKT/mTOR pathway, thereby inhibiting autophagy.

Keywords IL-17A, COPD airway remodelling, Mouse bronchial fibroblasts, Autophagy

Abbreviations

AKT	Protein kinase B
AP	Autophagosome
AR	Airway remodelling
Beclin-1	Becn1 gene
BSA	Bovine serum albumin
CCL20	CCL20
COPD	Chronic obstructive pulmonary disease
DAPI	Diamidine phenyl indole
ELISA	Enzyme-linked immunosorbent assay
IL-17A	Interleukin-17A
IL-1β	Interleukin-1β

Department of Respiratory and Critical Care Medicine, Affiliated Hospital of Zunyi Medical University, Guizhou 563003, China. ✉email: tingding2024@163.com; ouyangyao@zmu.edu.cn

IL-17RA	Interleukin-17A receptor
IL-6	Interleukin-6
LC3	Microtubule-associated protein 3
MBFs	Mouse bronchial fibroblasts
MOI	Multiplicity of infection
mTOR	Mammalian target of rapamycin
OD	Optical density
p-AKT	Phosphorylated protein kinase B
PBS	Phosphate-buffered saline
PI3K	Phosphatidylinositol 3-kinase
p-mTOR	Phosphorylated mammalian target of rapamycin
p-PI3K	Phosphorylated phosphatidylinositol 3-kinase
P62	Sequestosome 1, p62/SQSTM1
PVDF	Polyvinylidene fluoride

Background

COPD continues to increase the global health burden[1]. The disease is a heterogeneous pulmonary state that causes persistent progressive aggravation of airflow limitation[2]. Chronic inflammation, damage to airway epithelial cells, extracellular matrix (ECM) glycoprotein deposition, hyperplasia of airway smooth muscle cells, smoking, and genetic factors can lead to airway wall remodeling. Recent studies have shown that the new subtype of Th 17 cells is involved in the pathogenesis of COPD. IL-17A is an important factor secreted by Th 17 cells. IL-17A binds to IL-17RA, which can mediate the aggregation of neutrophils and promote the release of inflammatory factors by various cells, thus causing inflammatory diseases[3,4].Studies from Abdel-Magid proposed inhibiting interleukin 17A binding to the interleukin 17A receptor to treat inflammatory diseases[4]. Binding of IL-17A to its receptor can activate several signal transduction pathways, such as: NF-κ B, PI3K, AP1, and MAPK. These activities lead to the secretion of various pro-inflammatory cytokines, including IL-1 β, IL-6, IL-8, TNF, GCSF, PGE 2 and IFN- γ as well as many other chemokines and effectors[5].

Studies have shown that elevated IL-17A can be associated with small airway fibrosis in COPD patients and that inhibition of IL-17A can improve airway inflammation and fibrosis[6]. Bronchial fibroblasts are the main effector cells involved in airway remodelling. Fibroblasts are activated by inflammatory factors, leading to increased bronchial fibroblast proliferation, increased synthesis of extracellular matrix (ECM) components such as fibronectin and collagen, and airway remodelling[7]. The synthesis and decomposition of the ECM in the normal airway are in dynamic equilibrium, and the degradation of the ECM requires autophagy. Autophagy is a kind of cellular metabolic process that mainly refers to the degradation of lysosomes to form cell structures (organelles, nucleic acids, proteins and other biological macromolecules) and is an important defence and protection mechanism in the body[8].

Autophagy is a unique life phenomenon of eukaryotic cells. Autophagy uses lysosomes to degrade self-damaged cytoplasm and organelles. The degradation products can be used for energy generation, new protein and plasma membrane synthesis for cell metabolism and the renewal of aging damaged cell components, and maintain cell survival, differentiation, development and internal environment homeostasis.

Activation of autophagy requires the involvement of a series of autophagy-related proteins and cytokines. Bcl-2 binding to Beclin-1 inhibits the formation of the autophagic core complex and thereby regulates autophagy activation. Protein kinase B (AKT) is a serine/threonine protein kinase that is an important regulatory site of cell proliferation, differentiation, apoptosis and senescence. Moreover, the mammalian target of rapamycin (AKT)/mTOR pathway is also an important classical autophagy pathway[9].

The mTOR binds to and catalyzes phosphorylation of multiple targets, such as S6K1,4E-BP1, Akt, PKC, IGF-IR, and ULK 1, thereby regulating protein synthesis, nutrient metabolism, growth factor signaling, cell growth and migration, and regulation of autophagy.mTORC1 Is activated by multiple stimuli (e.g., growth factors, nutrients, energy, and stress signaling), and basic signaling pathways (e.g., PI3K, MAPK, and AMPK), and after mTORC1 activation, the anabolic processes are promoted by phosphorylation of the downstream effectors S6K and 4E-BP, such as protein, lipid, and nucleotide synthesis, while inhibiting the catabolic program by ULK 1, which leads to autophagy inhibition.

The enhancement or decrease in autophagy in COPD is controversial and may be related to differences in the selected models, cell classes and research methods[10–12]. Several studies have shown that IL-17A is associated with autophagy[13–15]. It has also been shown that IL-17 induced autophagy promotes mitochondrial dysfunction and fibrosis in bronchial fibroblasts from both non-asthmatic and severe asthmatic subjects[16]. While there are fewer narratives in COPD disease.

In addition, studies of skin keratinocytes have shown that IL-17A promotes CCL20 and IL-8 production through PI3K/Akt/mTOR inhibition of autophagy via the TOR pathway[17]. In lung fibroblasts, LPS also inhibited autophagy through the PI3K/Akt/mTOR pathway, thus participating in the progression of pulmonary fibrosis[18], which fully demonstrates the important role of the PI3K/Akt/mTOR axis in chronic inflammation and fibrosis. Airway remodelling in COPD patients occurs mainly through small airway fibrosis rather than pulmonary fibrosis. Whether IL-17A can inhibit autophagy in bronchial fibroblasts during COPD airway remodelling is currently unknown. Therefore, this study aimed to establish a mouse model of COPD to test whether IL-17A regulates airway remodelling in COPD through the PI3K/AKT/MTOR pathway by upregulating and downregulating IL-17RA in MBFs, providing novel targets for the treatment of COPD.

Materials and methods

Establishment of airway remodelling in COPD mice

This study was approved by the Animal Ethics Committee of Zunyi Medical University (ethical review number: KLLY (A)-2021-040). There was no clinical trial involved, so there was no clinical trial number. The source of mice used in the study from Hunan SJA Laboratory Animal Co., Ltd. Six- to eight-week-old male SPF-grade C57BL/6J mice (animal licence number: SCXK (Xiang) 2019-0004) were selected for adaptive feeding (23–26 °C, relative humidity 55–70%). The temperature and humidity of the experimental environment, as well as the equipment and reagents used in the experiment were strictly controlled to ensure the consistency of the experiment. All manipulations were performed by the same experimenter.

Studies have confirmed that the plasma IL-1β content in COPD patients is elevated, and IL-1β is significantly upregulated in an in vitro COPD model. COPD models are commonly created using a smoking method; however, considering the direct injection of IL-1β into the airway, which offers characteristics such as rapid molding time, a high mouse survival rate, and the stability of the constructed COPD model, this experiment aims to clarify the role of IL-17A in COPD airway remodeling, utilizing the methods described by Yanagisawa et al.[4]. Airway injection with high expression of IL-1 β, after adenovirus vector delivery of IL-1 β to the airway of mice, its expression is limited to airway epithelial, IL-1 β limited to the airway induced airway fibrosis but not emphysema changes, and similar to the pathological characteristics of COPD patients. Use purified negative control virus (Ad-LacZ) as control group. 3MA is an inhibitor of autophagy. In this experiment, we aimed to observe changes in COPD mice after autophagy inhibition. So thirty-two male mice were randomly divided into four groups: Ad-LacZ (Ad-LacZ control virus airway injection+PBS solution intraperitoneal injection), Ad-LacZ+3MA (Ad-LacZ control virus airway injection+3MA solution intraperitoneal injection), Ad-IL-1β (IL-1β adenovirus airway injection+PBS solution intraperitoneal injection) and Ad-IL-1β+3MA (IL-1β adenovirus airway injection+3MA solution intraperitoneal injection).

According to the method of airway virus injection established by Hashimoto et al.[19], mice at approximately 7 weeks of age were weighed and injected with the anaesthetic drug (1.2% tribromoethanol) at a dose of 0.2 mL/10 g. The median neck in the supine position was disinfected, the skin was cut to expose the trachea, and the prepared virus was inhaled with a 1 ml syringe. The needle was kept at a 45° angle to the trachea, and the virus was injected parallel to the trachea. Ad-LacZ airway injection was required in the Ad-LacZ group and in the Ad-LacZ+3MA group, while the Ad-IL-1β group and the Ad-IL-1β+3MA group were injected with Ad-IL-1β. After the neck skin was sutured, the mice were placed on an animal insulation table. Food and drinking water were provided in the animal room, and the bedding material was replaced quickly. After 7 days, the prepared 3MA solution (30 mg/kg) was injected intraperitoneally into the Ad-LacZ+3MA and Ad-IL-1β+3MA groups, and the other two groups were injected intraperitoneally with PBS. Serial injections were administered for 6 days, after the mice were sacrificed, the lung tissue and serum/plasma were collected on day 7.

Pulmonary function measurement

After adjusting the pulmonary function instrument on day 14, the COPD mice were anaesthetized with 0.1% tribromoethanol (intraperitoneal injection of 0.2 mL/10 g). In the supine position, the median skin of the neck was cut, a "T" incision was made on the trachea, the tracheal tube was inserted into the trachea, the trachea was secured with a No. 4 suture, the pulmonary function instrument was connected, the $FEV_{0.1}$ and FVC were measured, and the $FEV_{0.1}$/FVC was calculated. At the end of the measurement, the mouse was sacrificed (the right hand grasped the root of the tail and lifted it up, put it on the cage cover or other rough surface of the mouse, pressed the head and neck down gently with the left thumb and index finger, and the right hand grasped the root of the tail and pulled back and upward, causing cervical dislocation, the spinal cord was severed from the brainstem, and the experimental animal died immediately, no suffering was experienced, no chemical was used.) Then the whole lungs of the mice were removed and washed with saline several times. Lung tissue of an appropriate size was collected from the middle part of the left lung. Paraffin sections were fixed with 4% PFA and 3% glutaraldehyde. The remaining tissues were stored in a − 80 °C freezer for WB and ELISA analysis.

Slice preparation

Tissue samples were fixed in 4% paraformaldehyde for 48–72 h, and subsequently rinsed with running tap water for 24 h. Next, a graded alcohol dehydration treatment was performed, successively using 50%, 70%, 80%, 95%, and 100% alcohol. After that, the samples were fixed in xylene I and xylene II each for 30 min, and then cooled in liquid paraffin to form a paraffin block. Next, the tissues were cut into sections, then they were then deparaffinized the following day using two sequential 5 min washes in fresh xylene and rehydrated in graded ethanol baths (100%, 90%, 70%, 50%) and then washed 3 times with distilled water.

Serum collection

After constructing the model, blood from the eye was harvested and left at room temperature (this process involves gently pinching the mouse eye with forceps), and the upper serum was isolated. Following euthanasia of the mice, the lung tissue was collected.

HE staining

The slices were subjected to Harris hematoxylin staining for 3–8 min and subsequently washed with water. Next, the sections were immersed in 1% hydrochloride alcohol for differentiation for several seconds and rinsed again with water. To restore the blue color, the sections were placed in 0.6% ammonia and then washed with running water. Subsequently, the sections were placed in an eosin dye solution for staining for 1–3 min. After staining, the sections were sequentially dehydrated in an alcohol gradient. After removing the slices from xylene and drying them slightly, they were sealed using neutral gum.

Immunohistochemistry (IHC)

Following the completion of paraffin embedding, slicing, and antigen thermal repair, IHC experiments were conducted to detect IL-17A levels within each group. The tissue samples were thoroughly washed three times with PBS and then incubated with goat serum for one hour at room temperature (RT) to block nonspecific binding sites. Subsequently, the samples were incubated overnight at 4 °C with primary antibodies specific for IL-17A diluted at a ratio of 1:200. After another round of PBS washes, a working solution of HRP-labelled secondary antibodies was applied and incubated for one hour at RT. Following color development using DAB at RT for 1–10 min (in the dark), the slices were washed with distilled water for 30 min. Finally, the sections were sealed with neutral resin and observed under a microscope for analysis.

Masson staining

Weigert staining solution was applied to the sample for 8 min. Subsequently, the differentiation treatment was performed using an acidic ethanol differentiation solution for 15 s with slight washing after differentiation. Next, the sample was placed in Masson blue solution for 5 min and washed after completion. Next, staining was performed using magenta staining solution for 5 min. Then, the samples were washed in mild acid working solution for 1 min. Subsequently, the samples were washed with a phosphorolybdic acid solution for 1 min and then with a weak acid working solution. Next, the samples were subjected to aniline blue staining for 2 min and washed again with weak acid for 1 min. After completing the above steps, the transparent dehydration stage was started. First, 95% ethanol was used for rapid dehydration for 2–3 s, and the samples were dehydrated with absolute ethanol 3 times, each for 5–10 s. Next, xylene was used to make the sections transparent three times for 1–2 min each. Finally, the samples were secured using a neutral gum.

Immunofluorescence

Antigen retrieval was initially carried out using citrate buffer. Subsequently, tissue penetration was achieved by incubation with 0.3% Triton-X 100 diluted in PBS for 10 min, followed by blocking with 5% BSA for 30 min. The tissues were then incubated with primary antibodies specific for LC3 and vimentin (each diluted 1:200) in PBST at 4 °C for a period of one night. On the subsequent day, the slides were washed 4 times for 5 min each with 0.2% PBST. This was followed by incubation with species-specific fluorescent secondary antibodies (Cy3 diluted 1:200 and Alexa Fluor 488 diluted 1:100) in blocking solution for 45 min at RT. The slides were washed again for 15 min with 0.2% PBST, and this process was repeated 3 times before they were washed with 10 mM Tris–HCl for 10 min. Finally, the tissue slices were mounted using Mowiol and DAPI.

TEM observation of AP in lung tissue

The tissue was prefixed with 3% glutaraldehyde at 4 °C, followed by a second fixation with 1% osmium tetroxide. After hydrating with acetone and mixing with pure acetone and embedding agent 3:1, 1:1 and 1:3, the lung tissue was thoroughly soaked, and the lung tissue was thoroughly embedded with embedding agent; the final section thickness was cut to 60–90 nm; the tissue was stained at RT in uranium acetate medium for approximately 10–15 min and in lead citrate medium for approximately 1–2 min. Finally, TEM was used to find the right field of view, and pictures were taken.

ELISA

The steps for preparing lung tissue homogenates were as follows: First, approximately 1 g of lung tissue was washed with RT-treated PBS, and then 9 mL of RT-treated PBS containing 90 μL of protein phosphatase inhibitor was added on ice. Next, the processed samples were centrifuged for 10 min (4 °C, 5000 r/min), and the supernatant was collected and left for 2–3 h at RT. Then, the sample was precooled to 4 °C and centrifuged at 5000 r/min for 20 min, after which the supernatant was collected. To detect IL-17A/IL-6/CCL20 in lung tissue as well as CCL20 expression in serum, we used an ELISA kit with a double antibody sandwich method. The specific procedure was as follows: The purified mouse IL-17A/IL-6/CCL20 antibody was successively micro-placed onto a microtiter plate. Next, the antibodies were conjugated with HRP to generate solid-phase antibodies, which were sequentially added to the microplates. After conjugation with the HRP-labelled antibody, antibody-antigen-enzyme labelled antibody complexes were formed, which were then thoroughly washed and colored by the addition of the TMB substrate. TMB is converted to blue in response to the HRP enzyme. Notably, the concentration of the color was positively correlated with the added antibody content.

Western blot

Western blotting (WB) was used to detect IL-17RA/collagen I/collagen III/autophagy-related proteins and PI3K/AKT/mTOR-associated proteins in bronchial tissue or MBFs. The protein concentration was determined by a BCA protein assay kit. In this experiment, the appropriate gel concentration selected based on the protein molecular weight.12% gels for 14–20 kilodaltons (KD), 10% or 7.5% gels for 35–138 KD, and 6% for proteins above 250 KD. The proteins were separated by 6–12% sodium dodecyl sulfate-polyacrylamide gel electrophoresis and subsequently transferred to polyvinylidene fluoride membranes (Bio-Rad), which were subsequently blocked with Tris-buffered saline with Tween 20 (TBST) solution containing 5% skim milk at RT for 2 h. The corresponding primary antibodies (PI3K/p-PI3K/AKT/mTOR/p-mTOR/P62/Beclin-1/LC3A/B: CST Corporation, USA, anti-rabbit; collagen I/collagen III: Beijing Bioss Biotechnology Co., Ltd., anti-rabbit; IL-17A: Abcam, anti-rabbit) were diluted to a certain concentration (1:500) with blocking solution, and the final concentration of the internal reference primary antibody was 1:1000. The samples were then incubated overnight at 4 °C. After 3 washes with TBST, the membranes were incubated with secondary antibodies (Sigma, goat-anti-rabbit, 1:1000) at RT for 1 h. Finally, the samples were incubated with an enhanced chemiluminescence

(ECL) detection kit (Thermo Scientific Pierce™). we took cropped gels and blots images were collected (raw data attached in the supplementary file 3), and the band intensities were calculated by ImageJ.

Cell culture

We performed rapid and painless sacrifice on 4 mice. First, the necks of the mice were soaked for 5 min in 75% ethanol for disinfection. Subsequently, under strict sterile conditions, we cut the thorax of the mice and carefully removed the connective tissue around the trachea. We then used saline solution containing a 1% penicillin/streptomycin mixture to wash the residual blood and remove the heart tissue. Next, the lungs were moved to another Petri dish with saline. Then, the bronchial tissue was isolated from the lungs and cut into approximately 2–3 mm pieces, and 1 mL of collagenase was added to the finely minced tissue. The treated tissue was incubated in an incubator for 12 min, after which it was centrifuged (1200 r/min, 5 min). The deposits were collected and placed in culture bottles. After 24 h of incubation, the nonadherent cells were removed and cultured continuously for 3–5 days. In this study, we used primary fibroblasts.

Lentiviral transfection of MBFs

Tissue was digested using trypsin, and a cell suspension was prepared at concentrations ranging from 9×10^5/mL to 10×10^5/mL. Subsequently, 1 mL of cell suspension was seeded in six-well plates, and after 4–6 h, the adhesion and growth of the MBFs were observed by microscopy. The multiplicity of infection (MOI) for the MBFs was set to 30, which is the ratio of virus titre (virus volume/cell number). We calculated the desired viral volume from this formula. Lentiviruses containing anti-puromycin genes, including vector, OE, and sh viruses. RNA-seq libraries were sequenced using via Sanger sequencing. The paired-end sequenced raw reads were deposited in the NCBI-SRA database with the accession number PQ043210.1 (OE) [https://www.ncbi.nlm.nih.gov/search/all/?term=PQ043210.1], PQ043211 (sh) [https://www.ncbi.nlm.nih.gov/search/all/?term=PQ043211]. The lentivirus were dissolved on ice and mixed with 5 µL of protransfection enhancement solution, and 1 mL of medium was added. Subsequently, the original media was removed, and the virus-containing media were added and cultured continuously for 24–72 h. When green fluorescence appears under the microscope at 72 h or longer after transfection, we will use Cell Counting Kit-8 (CCK-8) reagent for rapid, highly sensitive detection of cell proliferation and cytotoxicity. CCK-8 reagent was used to observe and test the effect of different concentrations of puromycin, IL-17A, and rapamycin (Rapa) on MBFs.

Instruments and programs

For 50–200 nm sections SEM imaging, Optical inverted microscope (Model TMS-1015, OLYMPUS Company, Japan)were used, For TEM, ultrathin 70 nm sections were cut and deposited on 200 mesh support grids (JSM 7200F LV, JEOL, Japan).

Statistical analysis

The data were analysed using SPSS 22.0 software, and the images were analysed with Image Lab and mapped with GraphPad Prism. The data are presented as the means ± standard deviation ($\overline{x} \pm s$). One-way analysis of variance was used for multiple group comparisons, the least significant difference (LSD) test was used for equal variance, and Dunnett's T3 test was used for heterogeneity of variance. $P < 0.05$ was considered to indicate statistical significance.

Results

Pulmonary function testing in the COPD mice

Two weeks after COPD model establishment (n = 8), the FEV0.1/FVC (%) were lower in the Ad-LacZ+3MA (78% ± 8%, $P < 0.05$), Ad-IL-1β (72% ± 9%, $P < 0.05$), and Ad-IL-1β+3MA (78% ± 8%, $P < 0.05$) groups than in the Ad-LacZ group (94% ± 2%), suggesting that COPD mice have small airway obstruction (Fig. 1b).

Pathological findings of the COPD mice

After HE staining, microscopic observation revealed that the lung tissue structure of the Ad-LacZ group mice remained basically normal without significant inflammatory cell infiltration. However, the Ad-LacZ+3MA group exhibited thickening of the airway wall and smooth muscle. However, in the Ad-IL-1β group and the Ad-IL-1β+3MA group, a large accumulation of inflammatory cells was observed around the small airways in the lung tissue, accompanied by significant thickening of the bronchial wall and smooth muscle. These pathological changes were consistent with the characteristics of airway inflammation and remodelling in COPD patients (Fig. 1a). Further analysis by Masson staining revealed significantly increased collagen fibril production in the Ad-IL-1β (46.79 ± 7.7%) and Ad-IL-1β+3MA groups (43.95 ± 6.32%, shown by arrows) ($P < 0.05$). Notably, there was a significant difference between the Ad-IL-1 β+3MA group and the Ad-LacZ+3MA group (36.03 ± 5.46%) ($P < 0.05$) (Fig. 1c). These observations are all consistent with the characteristics of airway remodelling in COPD patients.

Collagen expression in the mouse airway

After WB detection, we observed the expression of collagen I and collagen III in the airways. Compared with that in the Ad-LacZ group, the collagen I expression in the Ad-LacZ+3MA group showed a certain trend, although this increase was not statistically significant ($P > 0.05$). However, a significant increase in collagen I expression occurred in the Ad-IL-1β and Ad-IL-1β+3MA groups ($P < 0.05$). Further comparison also revealed a significant increase in collagen I expression in the Ad-IL-1β+3MA group compared to that in the Ad-LacZ+3MA group ($P < 0.05$). Similarly, Collagen III expression was significantly greater in the Ad-LacZ+3MA, Ad-IL-1β, and Ad-IL-1β+3MA groups than in the Ad-LacZ group ($P < 0.05$). In the Ad-IL-1 β+3MA group, the expression

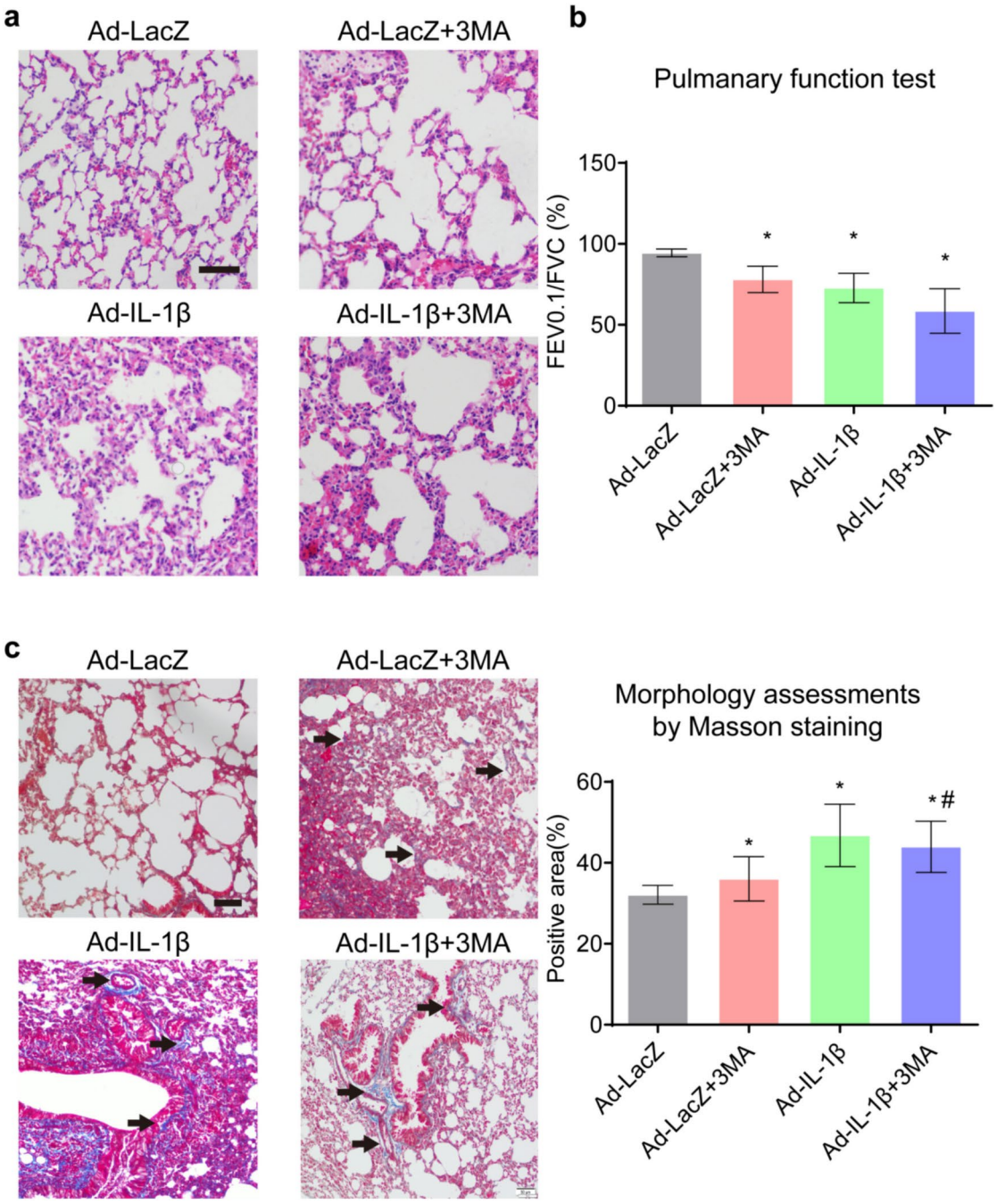

Fig. 1. Functional and morphological validation of COPD establishment of each group. (**a**) Morphology assessmemts by H&E staining. (**b**) Pulmonary function testing. c Morphology assessmemts by Masson staining (a. 400X; b. 400X). Data expressed as mean ± SEM from five independent experiments. $^{*}P < 0.05$ compared with the Ad-LacZ group. $^{\#}P < 0.05$ compared with Ad-LacZ+3MA group.

of Collagen III also increased significantly compared to that in the Ad-LacZ+3MA group ($P < 0.05$) (Table 1, Fig. 2a).

The expression of IL-17A, IL-6, and CCL20 in the mouse airway and of CCL20 in blood plasma

To test the expression level of IL-17A in lung tissue, we used two methods: ELISA and immunohistochemical staining. ELISA (Table 1, Fig. 2b) revealed that IL-17A expression levels were significantly greater in the Ad-IL-1β group than in the Ad-LacZ group ($P < 0.05$). Similarly, the results of immunohistochemical staining also showed that the percentage of IL-17A-positive cells was significantly greater in the Ad-IL-1β group than in the Ad-LacZ group ($P < 0.05$). To explore the expression of IL-6 and CCL20 in mouse lung tissue and CCL20 in plasma, we used ELISA. The experimental results showed that IL-6 expression increased in both the Ad-IL-1β group and the Ad-IL-1β+3MA group ($P < 0.05$); however, there were no statistically significant differences in

Groups	Ad-LacZ	Ad-LacZ+3MA	Ad-IL-1β	Ad-IL-1β+3MA
Collagen I/GAPDH	0.42 ± 0.17	0.57 ± 0.18	0.67 ± 0.22*	0.77 ± 0.13*#
Collagen III/GAPDH	0.83 ± 0.07	1.08 ± 0.26*	1.13 ± 0.28*	1.30 ± 0.20*#
IL-17A(pg/ml) by ELISA	449.1 ± 19.58	307.5 ± 36.45*	694.6 ± 24.00*	631.6 ± 80.92
IL-17A(%Area)by IHC	25.51 ± 2.27	20.46 ± 1.87*	32.67 ± 3.42*	25.80 ± 1.98
IL-6(pg/ml) by ELISA	468.10 ± 20.93	443.60 ± 23.15	891.20 ± 39.24*	780.30 ± 37.29*
CCL20(pg/ml) by ELISA in Lung	36.22 ± 8.17	31.82 ± 6.47	224.20 ± 21.56*	183.30 ± 10.29*
CCL20(pg/ml) by ELISA in plasma	27.66 ± 7.90	23.72 ± 3.84	137.10 ± 18.39*	64.19 ± 12.54*

Table 1. Content of collagen I/III and inflammatory factors in lung tissue ($\overline{x} \pm s$, n = 6). *$P < 0.05$ compared with Ad-LacZ group, #$P < 0.05$ compared with Ad-LacZ+3MA group.

IL-6 expression between the Ad-IL-1β group and the Ad-IL-1β+3MA group. Furthermore, CCL20 expression in both lung tissue and plasma was greater in the Ad-IL-1β and Ad-IL-1β+3MA groups than in the Ad-LacZ group ($P < 0.05$) (Table 1, Fig. 2c).

Expression of autophagy-related proteins in the mouse airways

We used a WB assay to explore the expression of autophagy-related proteins in the lung tissue. The experimental results showed that P62 expression increased in the Ad-LacZ+3MA, Ad-IL-1 β, and Ad-IL-1 β+3MA groups and that the ratio of Beclin-1 and LC3II/I decreased compared to that in the Ad-LacZ group ($P < 0.05$) (Fig. 3a). To more accurately determine the expression level of LC3 in the MBFs of the airway tissue, we used immunofluorescence (IF) double staining. With vimentin (green fluorescence in Fig) as a specific marker of MBFs, we were able to locate MBFs in airway tissue. Subsequently, we examined the expression of LC3 (shown in red fluorescence) in the cytoplasm of MBFs, with blue fluorescence representing the nucleus. Compared with those in the Ad-LacZ group, the LC3 expression in the Ad-LacZ+3MA group, Ad-IL-1β group and Ad-IL-1β+3MA group significantly decreased ($P < 0.05$) (Table 2, Fig. 3b).

Formation of the autophagosome (AP) within the mouse airways

APs in the airway were detected by TEM. After statistical analysis, we found that the AP of the Ad-LacZ+3MA (5.20 ± 1.30), Ad-IL-1β (4.60 ± 1.52), and Ad-IL-1β+3MA groups (3.60 ± 1.14) decreased significantly compared with that of the Ad-LacZ group (9.80 ± 1.79, $P < 0.05$) (Fig. 4a).

Expression of proteins involved in the PI3K/AKT/mTOR pathway in the mouse airways

After intraperitoneal injection of different concentrations of 3MA (0, 10, 20, 30, 40, or 50 mg/kg), the p-PI3K/PI3K ratio increased with increasing concentrations of 3MA. In particular, when the concentration of 3MA was 30 mg/kg, the ratio was significantly greater than that in the 0 mg/kg group ($P < 0.01$), and the survival rate of the mice at this concentration was relatively high. Therefore, we chose 30 mg/kg as the dose for the subsequent experiments (Fig. 5a). We analysed the expression of proteins involved in the PI3K/AKT/TOR pathway by using WB detection. The p-PI3K/PI3K, p-AKT/AKT, and p-mTOR/mTOR ratios were significantly greater in the Ad-LacZ+3MA, Ad-IL-1β and Ad-IL-1β+3MA groups than in the Ad-LacZ group ($P < 0.05$) (Table 2, Fig. 4b).

Isolation, culture, and identification of the MBFs

Primary MBFs were incubated in an incubator for approximately 2–3 days and exhibited a spindle or triangular pattern. By day 5, the MBFs began to grow together and increased significantly. By day 7, the number of MBFs increased further, and some of the actively growing MBFs were radial or arranged in parallel, reaching approximately 90% confluence. Therefore, the cells were subcultured on day 7 (Fig. 5b). The specific marker vimentin of MBFs was identified by immunofluorescence. A filament or cloud-like green fluorescence signal, which indicates the expression of vimentin, was observed in the cytoplasm of the MBFs, which indicates that the MBFs were highly pure and were successfully cultured (Fig. 5c).

Identification of the optimal concentration and duration of IL-17A intervention in MBFs

After the CCK-8 assay, we explored the effect of different concentrations of IL-17A (5 ng/mL, 10 ng/mL, 20 ng/mL, 40 ng/mL and 80 ng/mL) on the stimulation of MBFs within 24 h. Compared with those in the control group, the OD values in the 10 ng/mL group were significantly greater ($P < 0.05$). However, the OD decreased with increasing IL-17A concentration. This indicates that the most significant growth promotion effect of MBFs occurred at an IL-17A concentration of 10 ng/mL. Therefore, we concluded that the optimal concentration of IL-17A for the treatment of MBFs is 10 ng/mL. The effects of 10 ng/mL IL-17A stimulation for 12 h, 24 h, 48 h and 72 h on MBFs were also explored using the CCK-8 method. Compared with the control group, the IL-17A-treated for 24 h group exhibited the greatest increase in the OD and proliferation of the MBFs ($P < 0.01$); therefore, 24 h was the best time for IL-17A-mediated effects on the MBFs (Supplementary Fig. 1a).

Optimal concentration and duration of Rapa intervention in MBFs

After performing the CCK-8 assay, we explored the effect of Rapa at different concentrations (0.5 μmol/L, 1 μmol/L, 2 μmol/L, and 4 μmol/L) on the stimulation of MBFs within 24 h. With increasing Rapa concentration, the survival rate of the MBFs gradually decreased: 80.23 ± 0.06%, 67.92 ± 0.08%, 62.72 ± 0.05%, and 35.04 ± 0.6%,

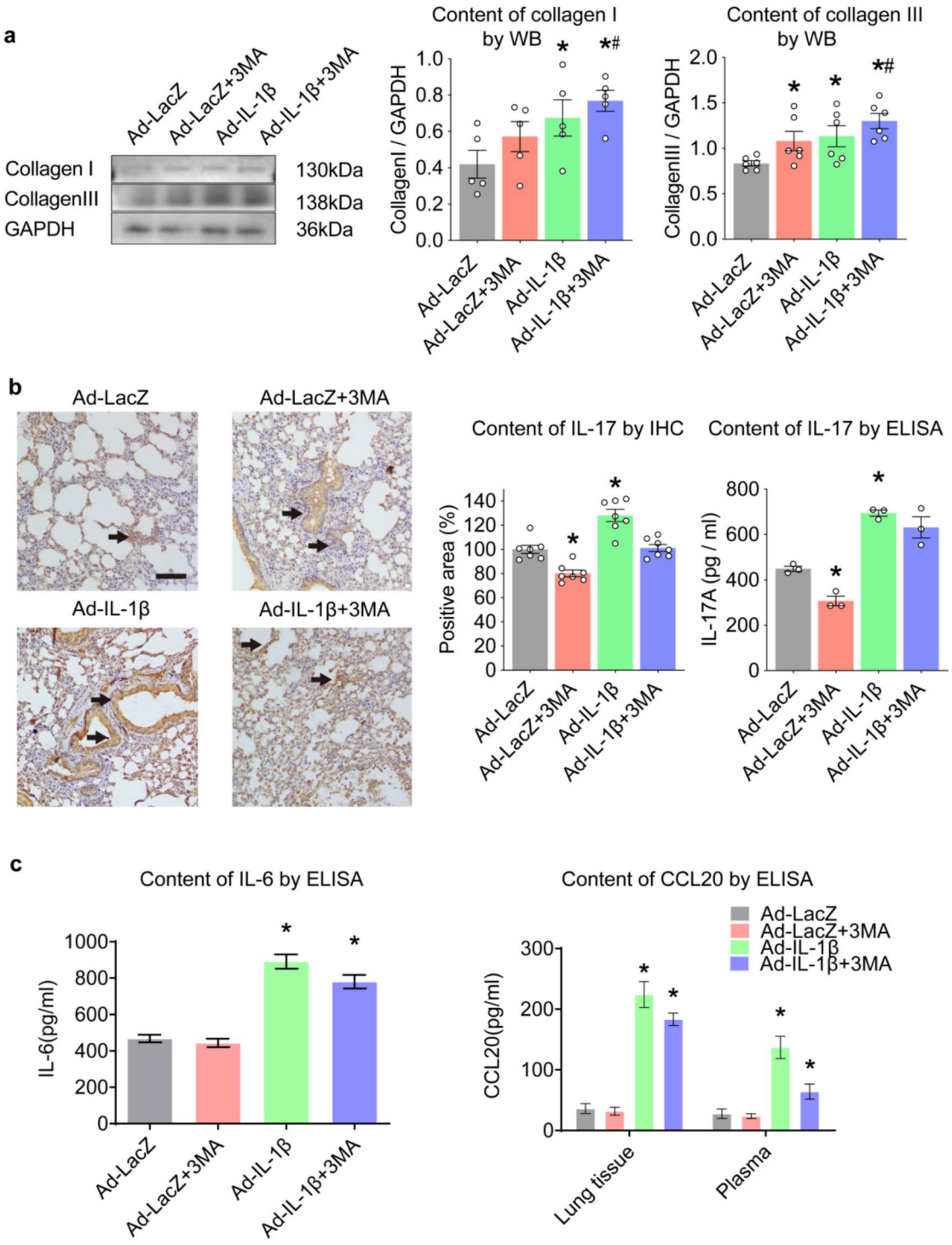

Fig. 2. Identification of collagen I/III in the airways and inflammatory factors in the lung. (**a**) Content of collagen I/III in the airways. (**b**) Identification of IL-17 by IHC&ELISA in lung. (**c**) IL-6 & CCL20 expression in lung. Data expressed as mean ± SEM from five independent experiments. $^{*}P < 0.05$ compared with Ad-LacZ group, $^{\#}P < 0.05$ compared with Ad-LacZ+3MA group.

respectively. Note that the changes in the viability of the MBFs were not significant at concentrations ranging from 0.5 to 1 μmol/L but became apparent at concentrations ranging from 2 to 4 μmol/L. Compared with that in the control group, the inhibitory effect of Rapa at 2 μmol/L on MBFs was more stable ($P < 0.05$). Therefore, we concluded that the optimal concentration of Rapa for the treatment of MBFs is 2 μmol/L. Then, we further examined the effect of 2 μmol/L Rapa on the survival of MBFs at 12 h, 24 h, 48 h and 72 h. Compared with the

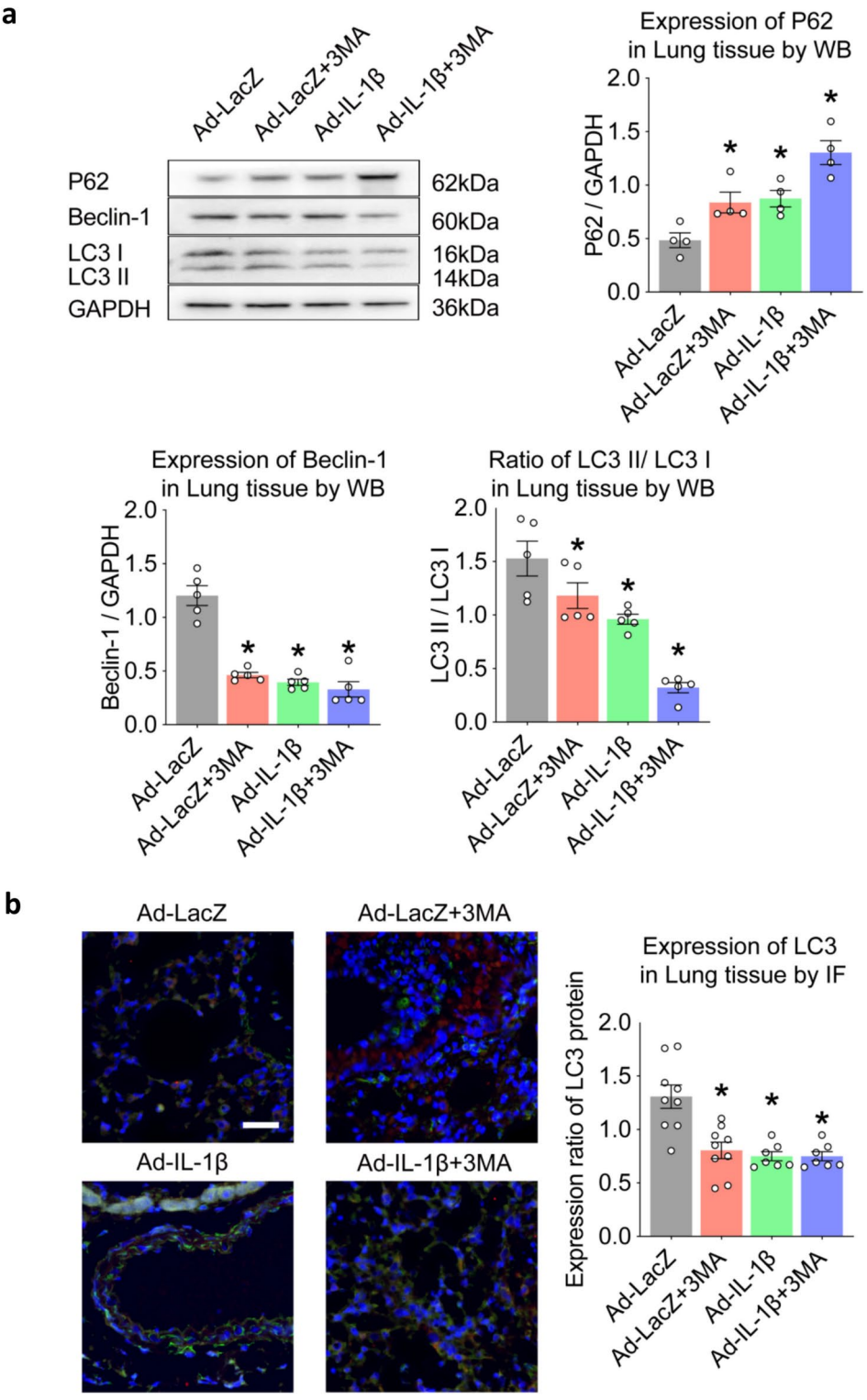

Fig. 3. Expression of autophagy-related proteins in the mouse airways. (**a**) Expression of P62/Beclin-1/ratio of LC3II/LC3 I in Lung tissue by WB. (**b**) Expression of LC3 in Lung tissue by IF, an immunofluorescence double staining of vimentin (green), LC3 (red), and nuclei (blue) was conducted on mice lung tissue. Scale bar: 50 μm. Data expressed as mean ± SEM from five independent experiments. $^{*}P < 0.05$ compared with Ad-LacZ group.

Groups	Ad-LacZ	Ad-LacZ+3MA	Ad-IL-1β	Ad-IL-1β+3MA
P62/GAPDH	0.49 ± 0.14	0.84 ± 0.19*	0.87 ± 0.16*	1.30 ± 0.22*
Beclin-1/GAPDH	1.20 ± 0.20	0.46 ± 0.05*	0.39 ± 0.07*	0.33 ± 0.16*
LC3II/LC3I	1.53 ± 0.36	1.18 ± 0.27*	0.96 ± 0.10*	0.32 ± 0.11*
Expression rate of LC3II	1.37 ± 0.28	0.76 ± 0.21*	0.72 ± 0.16*	0.69 ± 0.20*
AP	9.80 ± 1.79	5.20 ± 1.30*	4.60 ± 1.52*	3.60 ± 1.14*
p-PI3K/ PI3K	0.68 ± 0.15	0.97 ± 0.18*	1.17 ± 0.19*#	1.31 ± 0.10*#
p-AKT/AKT	0.57 ± 0.08	0.93 ± 0.07*	1.11 ± 0.12*#	1.62 ± 0.24*#
p-mTOR/mTOR	0.65 ± 0.13	1.47 ± 0.28*	1.84 ± 0.13*#	2.05 ± 0.42*#

Table 2. Content of autophagy-related proteins in the mouse airways ($\overline{x} \pm s$, n = 6). *$P < 0.05$ compared with Ad-LacZ group, #$P < 0.05$ compared with Ad-LacZ+3MA group.

control group, the results showed, compared with the Control group, the 24 h Rapa intervention inhibited MBFs most significantly ($P < 0.01$) (Supplementary Fig. 1b).

Identification of the optimal concentration and duration of purinomycin treatment in MBFs

The OD of different concentrations of purinomycin (0.5 μg/mL, 1 μg/mL, 2 μg/mL, 4 μg/mL, 8 μg/mL, and 16 μg/mL) and viability were calculated by the CCK-8 test. The viability at each concentration was 83.50 ± 3.64%, 79.01 ± 5.30%, 66.67 ± 0.44%, 47.26 ± 10.70%, 9.72 ± 1.76%, and 6.38 ± 0.37%, respectively. Notably, the survival rate decreased significantly at 4 μg/mL ($P < 0.05$), so 4 μg/mL was chosen as the appropriate concentration for cell screening. Furthermore, we examined the effect of 4 μg/mL purinomycin on MBF survival at different time points (12 h, 24 h, 48 h, and 72 h). The survival rates at each time point were 73.87 ± 6.27%, 40.07 ± 3.99%, 8.70 ± 1.30%, and 8.05 ± 0.92%, respectively. At 48 h, the cell survival rate was reduced to meet the experimental requirements. Therefore, 48 h was chosen as the intervention time for purinomycin in subsequent experiments (Fig. 5c).

Lentivirus infection of MBFs

Lentiviruses modified with the puromycin resistance gene (with a green fluorescent label) were used to transfect MBFs. From left to right, the results after transfection of MBFs with empty (Vector), overexpression (OE), and silenced (sh) viruses are shown. The fluorescence of the cells was finally observed and recorded at 72 to 96 h and even longer after transfection (Supplementary Fig. 1).

Expression of IL-17RA and PI3K/AKT/mTOR pathway proteins and autophagy-related proteins in OE virus-transfected MBFs

After transfection of MBFs with OE virus, the expression level of IL-17RA was significantly greater in the OE group than in the NC and vector groups ($P < 0.05$), indicating that OE virus transfection upregulated the expression of IL-17RA (Supplementary Table 1, Fig. 6a). Further detection of PI3K/AKT/mTOR pathway proteins revealed no significant difference in phosphorylation between the OE group and the vector group, but the p-PI3K/PI3K, p-AKT/AKT, and p-mTOR/mTOR ratios were much greater in the vector+IL-17A and OE+IL-17A groups than in the vector/OE group ($P < 0.05$) (Supplementary Table 2, Fig. 6b). Moreover, the detection of autophagy-related proteins in MBFs revealed that the level of P62 increased in the OE+IL-17A group, while the expression of Beclin-1 and LC3II/I decreased compared with that in the OE group ($P < 0.05$). In the OE+Rapa group, the expression of P62 decreased, while the expression of Beclin-1 and LC3II/I increased ($P < 0.05$). P62 expression was increased in the OE+IL-17A group and the OE+IL-17A+Rapa group compared to that in the OE+Rapa group; however, the expression of Beclin-1 and LC3II/I was decreased ($P < 0.05$). Furthermore, compared with the Vector+IL-17A group, the OE+IL-17A group exhibited increased P62 expression and decreased Beclin-1 and LC3II/I expression ($P < 0.05$). These results suggest that IL-17A inhibits autophagy through the receptor IL-17RA and attenuates the Rapa-induced expression of autophagy proteins (Supplementary Table 3, Fig. 6c).

Expression of the IL-17RA and PI3K/AKT/mTOR pathway proteins and autophagy-related proteins in shV-transfected MBFs

We found that the expression level of IL-17RA was significantly lower in MBFs transfected with sh virus ($P < 0.05$) than in the normal NC and vector groups (Supplementary Table 4, Fig. 7a). Moreover, we also observed that sh-mediated virus transfection did not significantly affect the phosphorylation of PI3K/AKT/mTOR pathway proteins, but the phosphorylation of pathway proteins was enhanced by IL-17A in the Vector+IL-17A group ($P < 0.05$). However, in the sh+IL-17A group, although the p-AKT/AKT and p-mTOR/mTOR ratios increased ($P < 0.05$), these ratios were still lower than those in the vector+IL-17A group ($P < 0.05$) (Supplementary Table 5, Fig. 7b). Furthermore, detection of proteins involved in autophagy in MBFs revealed that the expression of P62 but not that of Beclin-1 or LC3II/I was upregulated in the sh+IL-17A group ($P > 0.05$). Upon Rapa addition, P62 expression was decreased in the sh+Rapa group, whereas the expression of Beclin-1 and LC3II/I was increased ($P < 0.05$). However, P62 expression was increased in the sh+IL-17A and sh+IL-17A+Rapa groups but decreased in the Beclin-1 and LC3II/I groups compared to that in the sh+Rapa group ($P < 0.05$). Notably, compared with that in the vector+IL-17A group, P62 expression in the sh+IL-17A group but increased in the Beclin-1 and

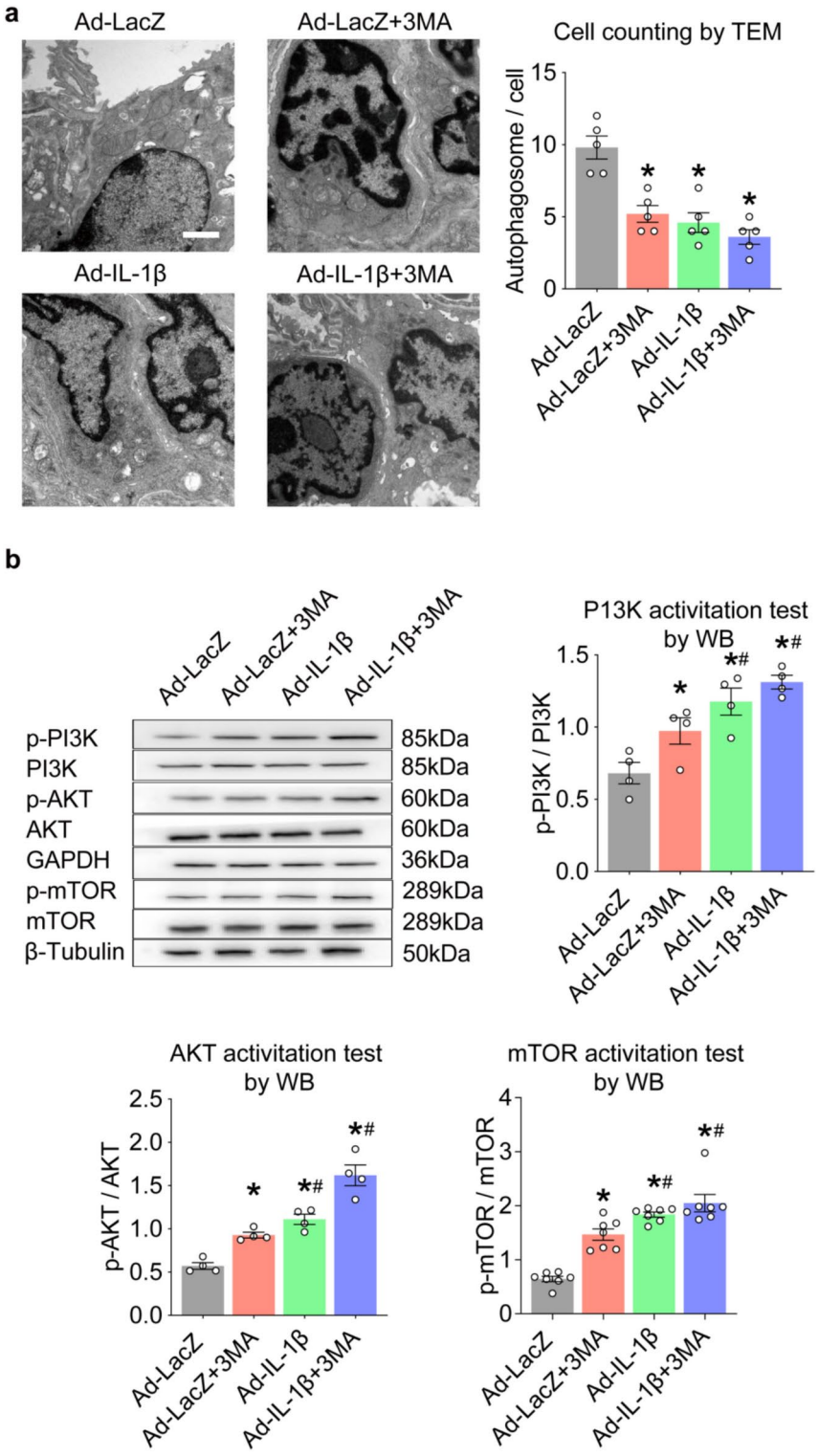

Fig. 4. Detection of autophagosomes and proteins associated with the PI3K/AKT/mTOR pathway in the mouse airways. (**a**) Counting of the autophagosomes in the mouse airways by TEM. (**b**) Expression of proteins associated with the PI3K/AKT/mTOR pathway. Data expressed as mean ± SEM from five independent experiments. $^{*}P < 0.05$ compared with Ad-LacZ group, $^{\#}P < 0.05$ compared with Ad-LacZ+3MA group.

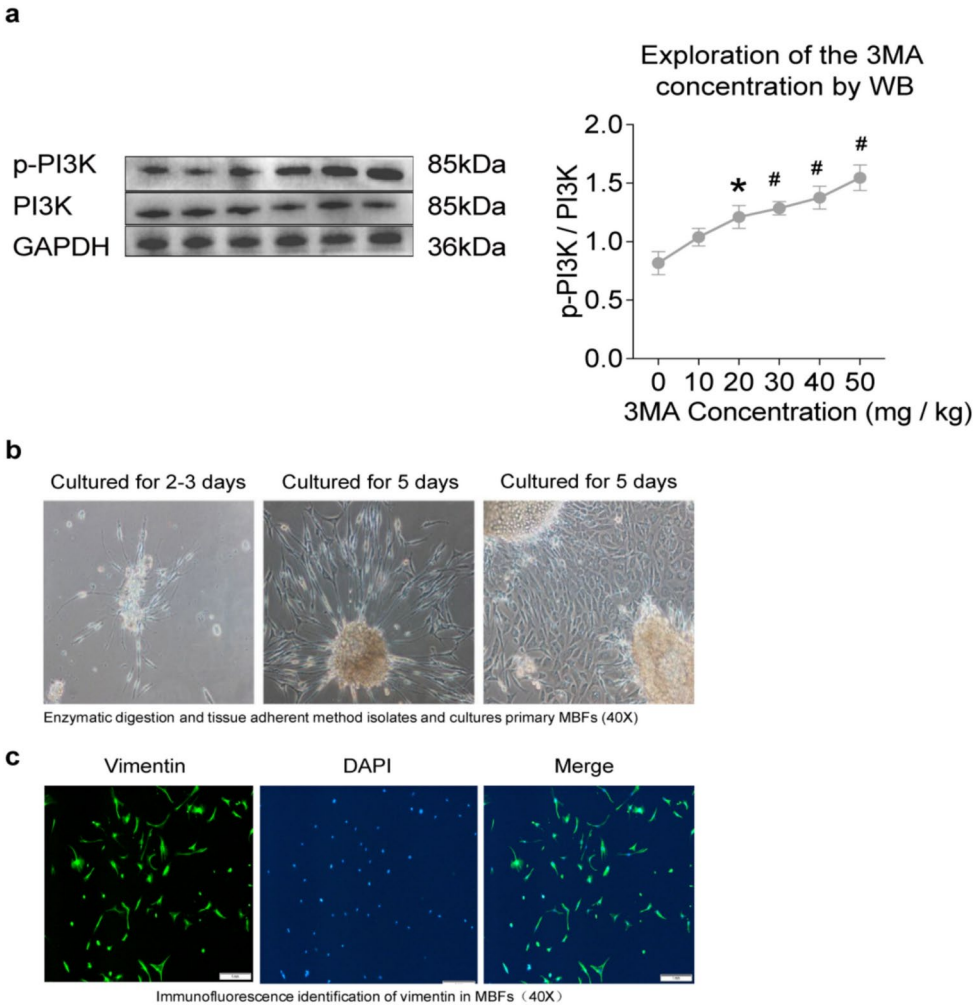

Fig. 5. A effect of different 3MA concentrations on p-PI3K/PI3K ratio and identification of the cultured MBFs. Data expressed as mean ± SEM from five independent experiments. $^{*}P < 0.05$ compared with 0 mg/kg group, $^{\#}P < 0.01$ compared with 0 mg/kg group. (**b**) Enzymatic digestion and tissue adherent method isolates and cultures primary MBFs. (**c**) Identification of the MBFs.

LC3II/I groups ($P < 0.05$). These results indicated that IL-17A had a significant effect on autophagy in sh virus-transfected MBFs (Supplementary Table 6, Fig. 7c).

Discussion

Chronic obstructive pulmonary disease (COPD) is a common disease that poses a serious threat to human health. Its main pathophysiological feature is persistent airflow limitation, and the underlying pathological mechanism is airway remodelling. In this process, bronchial fibroblasts play a key role, with significantly enhanced proliferation and migration activities, accompanied by increased synthesis of extracellular matrix (ECM) components such as fibronectin and collagen. Notably, the degradation process of the ECM relies on the autophagy mechanism, that is, cellular lysosomes degrade their own structures (such as organelles, nucleic acids, proteins and other biological macromolecules), which plays an important defense and protective role in the maintenance of body homeostasis[8]. Thus, decreased autophagy may play an important role in airway remodelling in COPD patients. Moreover, abnormal immune responses in the airway, whether innate immunity or adaptive immunity, are constantly driving the progression of COPD. The main characteristics of COPD are chronic changes in the small airways (F8). Therefore, the traditional smoking method was not used to construct the COPD model (this method mostly focuses on studying the pathogenesis of COPD pulmonary emphysema). However, airway injection of high-IL-1β adenoviral vectors was proposed by Hashimoto et al.[15]. In this approach, IL-1β is precisely delivered to the mouse airway via an adenoviral vector, and its expression is strictly restricted to the airway epithelium[12]. To further explore the role of autophagy in the pathogenesis of COPD, the phosphorylation of PI3K was regulated by injection of the autophagy inhibitor 3MA[15]. The experimental results showed that the p-PI3K/PI3K ratio gradually increased with increasing 3MA dose in the dose range of 0–50 mg/kg. The p-PI3K/PI3 ratio was significantly greater at the 30 mg/kg dose than at the 0 mg/kg dose, and the mice survived. Therefore, a dose of 30 mg/kg was used for comparison with the COPD model, aiming to clarify the

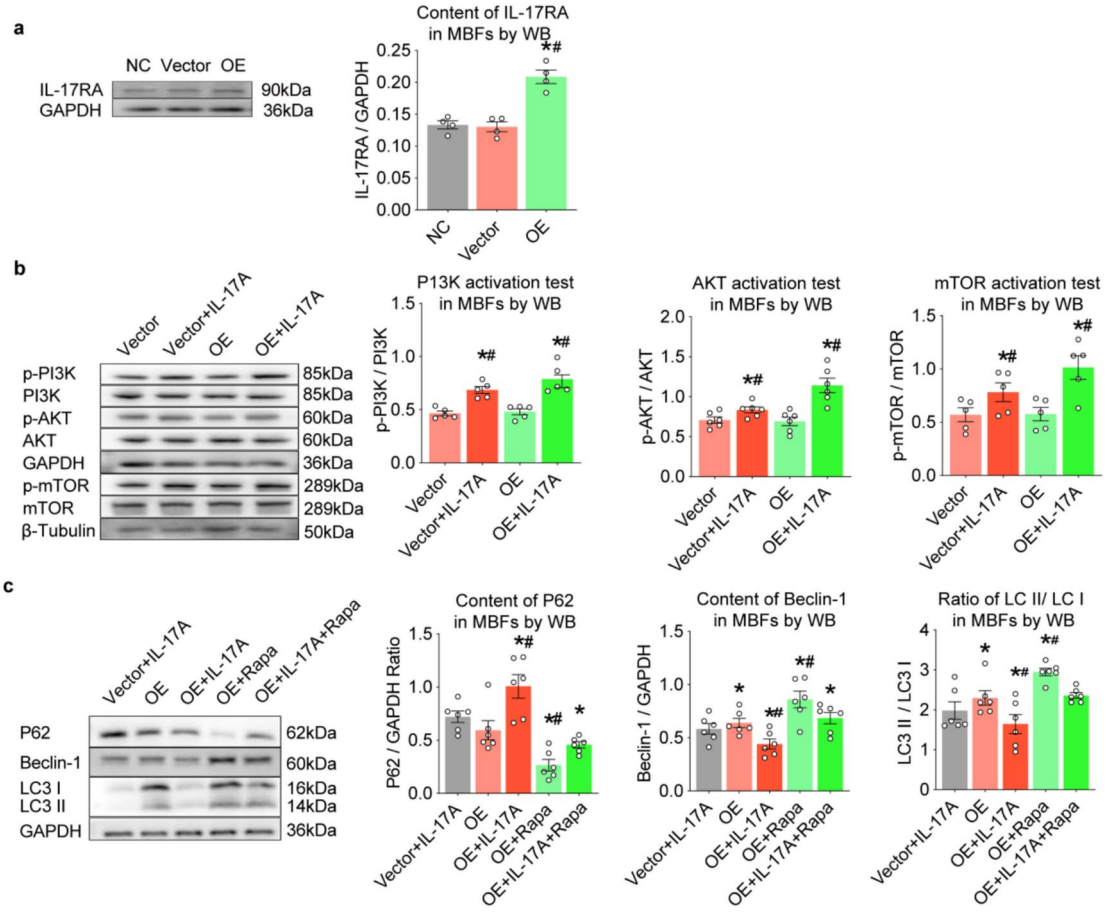

Fig. 6. Expression of IL-17RA and PI3K/AKT/mTOR pathway proteins and autophagy-related proteins in OE virus-transfected MBFs. (**a**) Content of IL-17RA in MBFs. (**b**) Content of PI3K /AKT/mTOR pathway proteins in MBFs. (**c**) Content of autophagy-related proteins in MBFs. Data expressed as mean ± SEM from five independent experiments. $^{*}P < 0.05$ compared with Vector group, $^{\#}P < 0.05$ compared with OE group.

association between the protein phosphorylation of pathway proteins and the change in autophagy level in the COPD mouse model.

We used a lung function instrument to accurately determine the forced expiratory volume (FEV 0.1) and forced vital capacity (FVC) of the mice within 0.1 s. By calculating the ratio of the two parameters, we could directly assess airway obstruction in mouse lung tissue[17,18]. We found that the FEV0.1/FVC ratio was significantly lower in the Ad-IL-1β group and Ad-IL-1β+3-MA group ($P < 0.05$), which suggested that small airways occurred in these two groups. Moreover, the results of HE staining further confirmed the presence of substantial inflammatory cell infiltration in the Ad-IL-1β group and the Ad-IL-1β+3MA group. However, Masson staining revealed the presence of numerous collagen fibres in both groups. These results all showed that the pulmonary pathological changes in the model mice were highly consistent with the characteristics of airway remodelling in chronic obstructive pulmonary disease (COPD), thus confirming the successful establishment of the airway remodelling model. However, the pulmonary function and histopathological changes in the Ad-IL-1 β group could not be reversed, even after the addition of 3MA. This is because IL-1 β adenovirus has been injected through the airway for 7 days, followed by 6 days of 3MA intraperitoneal injection, after which a mouse model of COPD lesions has been formed.

During the development of COPD, MBFs release abundant collagen, leading to epithelial cell fibrosis, which then triggers a vicious cycle of small airway stenosis and airflow obstruction[20]. In this study, WB revealed that the content of type I and type III collagen in the Ad-IL-1β group increased significantly, which further confirmed the phenomenon of increased collagen secretion during airway remodelling. In addition, studies have shown that peripheral blood and lung IL-17A+T cells and IL-17A levels increase in COPD patients and animal models, and these changes are closely related to the deterioration of lung function[21]. Moreover, mice deficient in the IL-17A gene were free from emphysema caused by CS exposure[22]. Studies show that IL-17 is capable of triggering cellular autophagic apoptosis[23]. As shown in the concept diagram we show, 3MA to inhibit the autophagic process results in reduced release of inflammatory factors, to explore whether this phenomenon is related to IL-17A, in the present study, we detected a significant increase in the secretion of IL-17A, CCL20, and IL-6 in the airway tissues of the Ad-IL-1β group by both ELISA and immunohistochemical staining. These results further

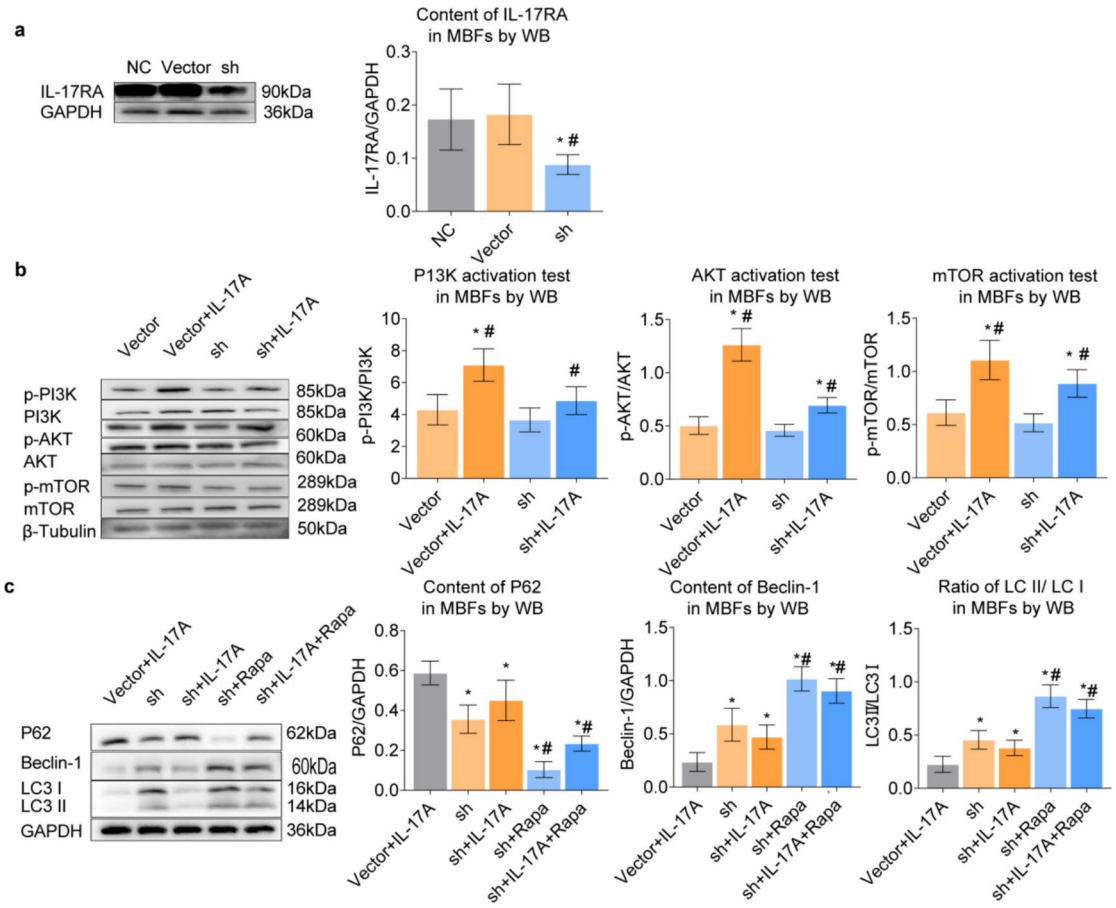

Fig. 7. Expression of IL-17RA and PI3K/AKT/mTOR pathway proteins and autophagy-related proteins in sh virus-transfected MBFs. (**a**) Content of IL-17RA in MBFs. (**b**) Content of PI3K/AKT/mTOR pathway proteins in MBFs. (**c**) Content of autophagy-related proteins in MBFs. Data expressed as mean ± SEM from five independent experiments. $^{*}P < 0.05$ compared with Vector+IL-17A group, $^{\#}P < 0.05$ compared with sh group.

confirmed that inflammation is indeed exacerbated in COPD airway remodelling model mice and that IL-17A is involved in this process.

Autophagy plays an important role in maintaining cellular homeostasis and is closely associated with autophagy-related genes (ATGs). Both the ATG5-12 and ATG8 binding systems regulate the function of autophagosomes. LC3, a well-known ATG protein, is homologous to ATG8. Its transformation process (i.e., the transition of LC3I to LC3II) and its degradation in the lysosome are key indicators of autophagy[24]. LC3II, a typical marker of autophagosomes, has been used to monitor the specificity of autophagy both in vitro and in vivo[25]. A decrease in the LC3 II/LC3 I ratio indicates that autophagy is inhibited. With P62 as a degradation substrate during autophagy, an increase in P62 usually indicates diminished autophagic activity, while a decrease in P62 may indicate autophagy activation. Beclin-1 plays a key role in regulating cellular autophagy and controlling autophagic activity through the activation of Vps[26]. A decrease in Beclin-1 expression indicated an inhibition of autophagy. Therefore, autophagy can be effectively detected by detecting key autophagy proteins and observing autophagosome formation[27]. In this study, we examined airway tissue from mice in the Ad-IL-1β group and found increased P62 expression, while the expression of Beclin-1 and the LC3 II/LC3 I ratio were decreased. TEM revealed a decrease in the number of autophagosomes in the Ad-IL-1β group. In addition, fluorescence double staining revealed that the LC3 content in MBFs in the Ad-IL-1β group was also reduced. These differences were all statistically significant compared to those in the Ad-LacZ group. These results suggest that the autophagy process is inhibited in the lung tissues of the airway remodelling model.

The PI3K/AKT/mTOR pathway plays a crucial role in regulating the level of cellular autophagy[28]. In fact, the inhibition of autophagy through the PI3K/Akt/mTOR pathway is a relatively classic pathway, which can be seen in a large number of chronic inflammatory diseases, such as pulmonary interstitial fibrosis, psoriasis, etc. Similarly, in studies of lung fibroblasts, it was shown that lipopolysaccharide also inhibited autophagy through the PI3K/Akt/mTOR pathway, thus participating in the progression of pulmonary interstitial fibrosis[29–31].

When this pathway is activated, the autophagy process is inhibited; however, when the pathway is inhibited, autophagy is enhanced[32]. We examined the activity by calculating the ratio of its potential active form to the protein. In this study, the p-PI3K/PI3K, p-AKT/AKT, and p-mTOR/mTOR ratios increased in the Ad-LacZ+3MA, Ad-IL-1β and Ad-IL-1β+3MA groups, suggesting that the PI3K/AKT/mTOR pathway was activated

in the COPD airway remodelling model. Moreover, the experimental results showed reduced autophagy in the airway tissue. Therefore, we hypothesized that activation of the PI3K/AKT/mTOR pathway may be an important mechanism for autophagy inhibition in a mouse model of COPD airway remodelling. 3MA as an autophagy inhibitor and can regulate PI3K phosphorylation levels. Found in this experimental study, 3MA As the p-PI3K / PI3K ratio gradually increased in the 0–50 mg/kg dose range, in the study of treated mice at 30 mg/kg and controlled with the Ad-LacZ model, the results supported the conclusion that 3MA increased the p-PI3K/PI3K ratio. However, the activation of this pathway was not observed in the Ad-IL-1β COPD model. This is because, in the in vivo experiments of IL-17A (immunohistochemistry and ELISA) for this study, compared to the Ad-LacZ control group, the number of IL-17A in the airways of mice treated with 3MA decreased. It is considered that the addition of 3MA may have led to a reduction in IL-17A. In the COPD group established with Ad-IL-1β, the increase in IL-17 was significant; however, after adding 3MA, the content of IL-17 was also significantly reduced, indicating that the establishment of COPD model may not be the most critical factor affecting the results. We know that IL-17 has an inhibitory effect on the PI3K-AKTmTOR pathway activation, so the impact of 3MA on IL-17 levels might indirectly result in the failure to observe the activation of the PI3K-AKTmTOR pathway in the in vivo experiment. This is a limitation of this experiment. In subsequent in vitro experiments, we have overexpressed the IL-17A to activate this pathway to observe the effect of 3MA. Combining the results from both parts, our conclusion can not be definitively stated as confirming that exogenous addition of 3MA leads to reduced autophagy due to the activation of the PI3K/AKT/mTOR pathway. Instead, we should acknowledge the limitations and incompleteness of the experiment. Future studies can further verify the relationship between autophagy inhibition and the pathway by adding other autophagy inhibitors or activators, as well as IL-17 activators.

Fibroblasts play a key role in airway remodelling in COPD[33]. Studies have shown that bronchial fibroblasts and lung fibroblasts are functionally different during damage repair processes. During the development of COPD, the destruction of the alveolar wall structure of the lung parenchyma occurs due to inflammatory stimulation, mainly resulting in changes in emphysema rather than obvious fibrosis. In contrast, bronchi exhibit altered fibroblast proliferation, bronchial wall thickening, fibrosis and structural remodelling[34]. Therefore, this study focused on the specific role of bronchial fibroblasts in airway remodelling. The primary MBFs used in the experiments were isolated from mouse lung tissue to investigate the effect of IL-17A on the PI3K/AKT/mTOR pathway and autophagy levels. The effect of different concentrations of IL-17A (5 ng/mL, 10 ng/mL, 20 ng/mL, 40 ng/mL, and 80 ng/mL) on MBFs was evaluated. The CCK-8 assay showed that the 10 ng/mL group had the highest OD value ($P<0.05$), while the OD value decreased as the concentration increased. This indicates that 10 ng/mL IL-17A promoted the most significant growth of MBFs. Therefore, we chose 10 ng/mL as the optimal concentration for IL-17A intervention in MBFs. Furthermore, to explore whether IL-17A could regulate autophagy in MBFs, we used the autophagy inducer Rapa as a control. MBFs were stimulated for 24 h with different concentrations of Rapa (0.5 μmol/L, 1 μmol/L, 1 μmol/L, 2 μmol/L, or 4 μmol/L), and cell viability was calculated using the CCK-8 method. The results showed that Rapa had an inhibitory effect on cell growth and that this effect was positively correlated with the reagent concentration. Compared with the control group, the 2 μmol/L group had the most significant stable inhibition of MBFs ($P<0.05$), and the survival rate met the experimental requirements. We used lentiviral-transfected MBFs and examined the expression of IL-17RA via WB. In the case of MBFs transfected with OE virus, we observed that the normal NC and vector groups did not show significant differences in IL-17RA expression, while the OE group showed significantly greater IL-17RA expression, which was significantly different from the first two groups ($P<0.05$). In the case of MBFs transfected with the sh virus, there was no significant difference in IL-17RA expression between the normal NC and vector groups, but the sh group showed a low IL-17RA expression level, which was significantly different from that of the other two groups ($P<0.05$). Taken together, these results indicate that the lentiviruses successfully transfected MBFs and induced the overexpression or silencing of IL-17RA.

The PI3K/AKT/mTOR pathway plays a crucial role in cellular physiology and pathological processes[35]. According to previous studies, increased phosphorylation of the PI3K/AKT/mTOR pathway is associated with increased IL-17A secretion in a mouse model of Sjogren's syndrome[36]. In animal models of psoriasis and dyslipidemia, TCM cooling blood and detoxification (a traditional Chinese medicine) can effectively inhibit the protein expression of PI3K, AKT, and mTOR and their phosphorylation and significantly reduce the secretion of IL-17A[37]. Furthermore, PM2.5 was able to increase IL-17A and activate PI3K/AKT/mTOR signaling in mouse lung tissue, subsequently inhibiting autophagy in bronchial epithelial cells[3]. Based on the above studies, we hypothesized that IL-17A may be associated with the activation of the PI3K/AKT/mTOR signaling pathway in MBFs (Fig. 8). Therefore, lentiviral transfection was used to overexpress or silence IL-17RA, and transfected MBFs were stimulated with IL-17A to examine the protein expression levels of PI3K, AKT, and mTOR by WB to determine the effect of IL-17A on the PI3K/AKT/MTOR pathway in MBFs. The results showed that after OE lentivirus-mediated overexpression of IL-17RA in MBFs, stimulation of the cells with IL-17A increased the p-PI3K/PI3K, p-AKT/AKT, and p-mTOR/mTOR ratios, and the p-PI3K/PI3K, p-AKT/AKT, and p-mTOR/mTOR ratios were greater in the OE+IL-17A group than in the Vector+IL-17A group. However, after silencing IL-17RA in MBFs with a sh lentivirus, phosphoprotein synthesis in the vector+IL-17A group was greater than that in the vector group, and the p-AKT/AKT and p-mTOR/mTOR ratios were greater in the sh+IL-17A group but lower than those in the vector+IL-17A group. These results suggest that IL-17A activates the PI3K/AKT/mTOR pathway in MBFs through its receptor, IL-17RA. Furthermore, we examined the changes in the expression of the autophagy-related proteins P62, Beclin-1, and LC3II/I by WB to clarify the effect of IL-17A on autophagy in MBFs. The experimental results showed that IL-17A inhibited the autophagy of the MBFs. Considering the above experimental results, we conclude that IL-17A promotes airway remodelling and accelerates the pathology of COPD by activating the PI3K/AKT/mTOR pathway and inhibiting autophagy.

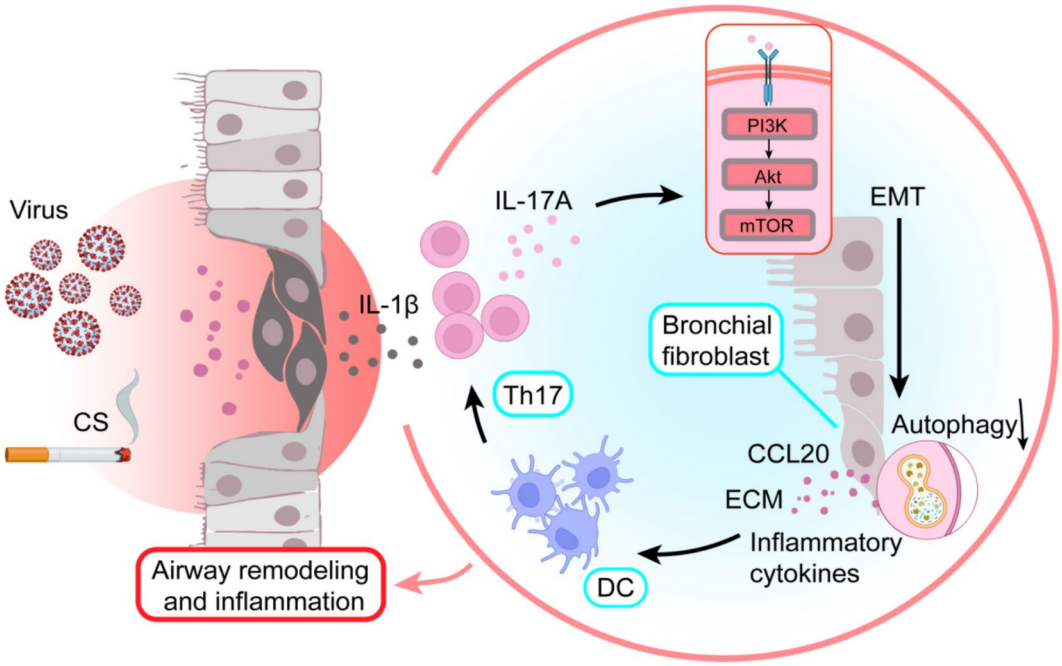

Fig. 8. Abstract graphic of IL-17A regulates airway remodelling in COPD through the PI3K/AKT/mTOR pathway.

Conclusions

Based on the in vivo and in vitro experiments described above, collagen hyperplasia and increased inflammatory factor levels were detected in the airways of COPD mice. This pathological change was caused by the binding of IL-17A to the receptor IL-17RA, which activates the PI3K / AKT / mTOR pathway, leading to the massive degradation of P62 during autophagy, the obvious decrease of Beclin-1, a key molecule controlling the autophagic activity, and the reduced transformation of the typical autophagosome marker LC3I to LC3II, thus reflecting the reduction of autophagy levels in bronchial fibroblasts, this process provides new insights into the pathogenesis of COPD.

Data availability

The paired-end sequenced raw reads were deposited in the NCBI-SRA database with the accession number PQ043210.1 (OE) [https://www.ncbi.nlm.nih.gov/search/all/?term=PQ043210.1], PQ043211 (sh) [https://www.ncbi.nlm.nih.gov/search/all/?term=PQ043211]. Data is provided within the manuscript or supplementary information files and is available from the corresponding author upon reasonable request.

Received: 20 August 2024; Accepted: 28 April 2025
Published online: 13 May 2025

References

1. Safiri, S. et al. Burden of chronic obstructive pulmonary disease and its attributable risk factors in 204 countries and territories, 1990–2019: Results from the Global Burden of Disease Study 2019. *BMJ* **378**, e069679 (2022).
2. Vijayan, V. K. Chronic obstructive pulmonary disease. *Indian J. Med. Res.* **137**(2), 251–269 (2013).
3. Cong, L. H. et al. IL-17A-producing T cells exacerbate fine particulate matter-induced lung inflammation and fibrosis by inhibiting PI3K/Akt/mTOR-mediated autophagy. *J. Cell Mol. Med.* **24**(15), 8532–8544 (2020).
4. Yanagisawa, H. et al. Role of IL-17A in murine models of COPD airway disease. *Am. J. Physiol. Lung Cell Mol. Physiol.* **312**(1), L122–L130 (2017).
5. Abdel-Magid, A. F. Inhibition of the Binding of Interleukin 17A with Interleukin 17A Receptor as a treatment for immune system and inflammation disorders, cancer, and neurodegenerative diseases. *ACS Med. Chem. Lett.* **15**(12), 2088–2090. https://doi.org/10.1021/acsmedchemlett.4c00532 (2024).
6. Wang, F. et al. IL-1β receptor antagonist (IL-1Ra) combined with autophagy inducer (TAT-Beclin1) is an effective alternative for attenuating extracellular matrix degradation in rat and human osteoarthritis chondrocytes. *Arthritis Res. Ther.* **21**(1), 171 (2019).
7. Christopoulou, M. E., Papakonstantinou, E. & Stolz, D. Matrix metalloproteinases in chronic obstructive pulmonary disease. *Int. J. Mol. Sci.* **24**(4), 3786 (2023).
8. Roscioli, E. et al. Airway epithelial cells exposed to wildfire smoke extract exhibit dysregulated autophagy and barrier dysfunction consistent with COPD. *Respir. Res.* **19**(1), 234 (2018).
9. Wu, N. et al. The anti-tumor effects of dual PI3K/mTOR inhibitor BEZ235 and histone deacetylase inhibitor Trichostatin A on inducing autophagy in esophageal squamous cell carcinoma. *J. Cancer.* **9**(6), 987–997 (2018).
10. Nachmias, N. et al. NLRP3 inflammasome activity is upregulated in an in-vitro model of COPD exacerbation. *PLoS ONE* **14**(5), e0214622 (2019).
11. Liang, G. B. & He, Z. H. Animal models of emphysema. *Chin. Med. J. (Engl.)* **132**(20), 2465–2475 (2019).

12. Botelho, F. M. et al. IL-1α/IL-1R1 expression in chronic obstructive pulmonary disease and mechanistic relevance to smoke-induced neutrophilia in mice. *PLoS ONE* **6**(12), e28457 (2011).
13. Wang, C., Feng, D., Dong, S., He, R. & Fan, B. Dysregulated circulating microRNA-126 in chronic obstructive pulmonary disease: linkage with acute exacerbation risk, severity degree, and inflammatory cytokines. *J. Clin. Lab Anal.* **36**(3), e24204 (2022).
14. Kitamura, H. et al. Mouse and human lung fibroblasts regulate dendritic cell trafficking, airway inflammation, and fibrosis through integrin αvβ8-mediated activation of TGF-β. *J. Clin. Invest.* **121**(7), 2863–2875 (2011).
15. Du, J. et al. PI3K inhibitor 3-MA promotes the antiproliferative activity of esomeprazole in gastric cancer cells by downregulating EGFR via the PI3K/FOXO3a pathway. *Biomed. Pharmacother.* **148**, 112665 (2022).
16. Ramakrishnan, R. K. et al. IL-17 induced autophagy regulates mitochondrial dysfunction and fibrosis in severe asthmatic bronchial fibroblasts. *Front. Immunol.* **11**, 1002. https://doi.org/10.3389/fimmu.2020.01002 (2020).
17. Bonnardel, E. et al. Determination of reliable lung function parameters in intubated mice. *Respir. Res.* **20**(1), 211 (2019).
18. Xiao, C. et al. Isoforskolin alleviates AECOPD by improving pulmonary function and attenuating inflammation which involves downregulation of Th17/IL-17A and NF-κB/NLRP3. *Front. Pharmacol.* **12**, 721273 (2021).
19. Hashimoto, M. et al. A critical role for dendritic cells in the evolution of IL-1β-mediated murine airway disease. *J. Immunol.* **194**(8), 3962–3969 (2015).
20. Paw, M. et al. Responsiveness of human bronchial fibroblasts and epithelial cells from asthmatic and non-asthmatic donors to the transforming growth factor-β1 in epithelial-mesenchymal trophic unit model. *BMC Mol. Cell Biol.* **22**(1), 19 (2021).
21. Le Rouzic, O. et al. Th17 cytokines: novel potential therapeutic targets for COPD pathogenesis and exacerbations. *Eur. Respir. J.* **50**(4), 1602434 (2017).
22. Li, D. et al. IL-17A promotes epithelial ADAM9 expression in cigarette smoke-related COPD. *Int. J. Chron. Obstruct Pulmon. Dis.* **17**, 2589–2602 (2022).
23. Wang, L. et al. IL-17A/IL-17RA reduces cisplatin sensitivity of ovarian cancer SKOV3 cells by regulating autophagy. *Nan Fang Yi Ke Da Xue Xue Bao* **40**(11), 1550–1556. https://doi.org/10.12122/j.issn.1673-4254.2020.11.03 (2020).
24. Runwal, G. et al. LC3-positive structures are prominent in autophagy-deficient cells. *Sci. Rep.* **9**(1), 10147 (2019).
25. Ma, L. et al. Cigarette and IL-17A synergistically induce bronchial epithelial-–mesenchymal transition via activating IL-17R/NF-κB signaling. *BMC Pulm. Med.* **20**(1), 26 (2020).
26. Maejima, Y., Isobe, M. & Sadoshima, J. Regulation of autophagy by Beclin 1 in the heart. *J. Mol. Cell Cardiol.* **95**, 19–25 (2016).
27. Kaur, S. & Changotra, H. The beclin 1 interactome: Modification and roles in the pathology of autophagy-related disorders. *Biochimie* **175**, 34–49 (2020).
28. Miricescu, D. et al. PI3K/AKT/mTOR signaling pathway in breast cancer: from molecular landscape to clinical aspects. *Int. J. Mol. Sci.* **22**(1), 173 (2020).
29. Liu, H., Mi, S., Li, Z., Hua, F. & Hu, Z. W. Interleukin 17A inhibits autophagy through activation of PIK3CA to interrupt the GSK3B-mediated degradation of BCL2 in lung epithelial cells. *Autophagy* **9**(5), 730–742 (2013).
30. Varshney, P. & Saini, N. PI3K/AKT/mTOR activation and autophagy inhibition plays a key role in increased cholesterol during IL-17A mediated inflammatory response in psoriasis. *Biochim. Biophys. Acta Mol. Basis Dis.* **1864**(5 Pt A), 1795–1803 (2018).
31. Tingting, X. et al. Lipopolysaccharide promotes lung fibroblast proliferation through autophagy inhibition via activation of the PI3K-Akt-mTOR pathway. *Lab. Invest.* **99**, 625–633 (2019).
32. Jiang, F. et al. Fluorofenidone attenuates paraquat-induced pulmonary fibrosis by regulating the PI3K/Akt/mTOR signaling pathway and autophagy. *Mol. Med. Rep.* **23**(6), 405 (2021).
33. Esnault, S. et al. Increased IL-6 and potential IL-6 trans-signalling in the airways after an allergen challenge. *Clin. Exp. Allergy* **51**(4), 564–573 (2021).
34. Dessalle, K. et al. Human bronchial and parenchymal fibroblasts display differences in basal inflammatory phenotype and response to IL-17A. *Clin. Exp. Allergy* **46**(7), 945–956 (2016).
35. Porta, C., Paglino, C. & Mosca, A. Targeting PI3K/Akt/mTOR signaling in cancer. *Front. Oncol.* **4**, 64 (2014).
36. Zeng, P. et al. PI3K/AKT/mTOR signaling pathway is downregulated by Runzaoling (RZL) in Sjögren's syndrome. *Mediat. Inflamm.* **2022**, 7236118 (2022).
37. Xie, X. et al. Liangxue Jiedu formula improves psoriasis and dyslipidemia comorbidity *via* PI3K/Akt/mTOR pathway. *Front. Pharmacol.* **12**, 591608 (2021).

Acknowledgements

The authors would like to thank Professor Yong Zhao ， Professor Xiaomin Yang and Dr. Sheng Liu for their support.

Author contributions

YOY conceived the project. YOY, TD, and SSZ coordinated the research and TD, and SSZ as co-first author. TD, SSZ, CJ, LYZ and YHG contributed to research protocol development. SSZ, XMR, and LYZ performed the practical research. GQH and YZL performed genotype validation after lentiviral transfection. SSZ, JC, and TD analysed the data and created the figure. TD wrote the manuscript. All authors reviewed the manuscript and approved the final version. All the authors have read and approved the final manuscript.

Funding

This work was supported by the National Natural Science Foundation of China (Grant No. 8206010332) and the Master Start-up Foundation of Zunyi Medical University (Grant No. YZ 201319).

Declarations

Competing interests

The authors declare no competing interests.

Ethics approval and consent to participate

All animal experiments were carried out in accordance with the principles of the Guidelines for the Care and Use of Animals and were approved by the Laboratory Animal Welfare & Ethics Committee of ZunYi Medical University. The animal research reports adhered to the ARRIVE guidelines.

Additional information

Supplementary Information The online version contains supplementary material available at https://doi.org/10.1038/s41598-025-00458-9.

Correspondence and requests for materials should be addressed to T.D. or Y.O.-Y.

Reprints and permissions information is available at www.nature.com/reprints.

Publisher's note Springer Nature remains neutral with regard to jurisdictional claims in published maps and institutional affiliations.